

## SHAPES OF TOPOLOGICAL RNA STRUCTURES

FENIX W.D. HUANG AND CHRISTIAN M. REIDYS\*

ABSTRACT. A topological RNA structure is derived from a diagram and its shape is obtained by collapsing the stacks of the structure into single arcs and by removing any arcs of length one. Shapes contain key topological information and for fixed topological genus there exist only finitely many such shapes. We shall express topological RNA structures as unicellular maps, i.e. graphs together with a cyclic ordering of their half-edges. In this paper we prove a bijection of shapes of topological RNA structures. We furthermore derive a linear time algorithm generating shapes of fixed topological genus. We derive explicit expressions for the coefficients of the generating polynomial of these shapes and the generating function of RNA structures of genus  $g$ . Furthermore we outline how shapes can be used in order to extract essential information of RNA structure databases.

## 1. INTRODUCTION

Pseudoknots have long been known as important structural elements in RNA [23]. These cross-serial interactions between RNA nucleotides are functionally important in tRNAs, RNaseP [11], telomerase RNA [20], and ribosomal RNAs [9]. Pseudoknots in plant virus RNAs mimic tRNA structures, and *in vitro* selection experiments have produced pseudoknotted RNA families that bind to the HIV-1 reverse transcriptase [22].

Since the prediction of general RNA pseudoknot structures is NP-complete [12], one frequently sticks to certain subclasses of pseudoknots, suitable for the dynamic programming paradigm [19, 17].

---

*Date:* Received: date / Accepted: date.

In [17] a folding algorithm, `gfold`, for one such class of RNA structures has been presented. This class consists of structures of fixed topological genus. The topological filtration of RNA structures has first been proposed by Penner and Waterman in [16] and later, as an application of the Matrix model in [14] and [2]. In [17, 1] a representation theoretic Ansatz is employed that traces back to Zagier [24]. [1] connects RNA shapes of fixed topological genus with Riemann’s moduli space.

RNA structures are represented as diagrams, that is as labeled graphs over the vertex set  $[n] = \{1, \dots, n\}$  with vertex degrees  $\leq 3$ , represented by drawing its vertices on a horizontal line and its arcs  $(i, j)$  ( $i < j$ ), in the upper half-plane, see Figure 1 (A). We assume the vertices to be connected by the edges  $\{i, i + 1\}$ ,  $1 \leq i < n$ , which are not considered to be arcs (but contribute to a nodes’s degree). Furthermore, vertices and arcs correspond to the nucleotides **A**, **G**, **U** and **C** and Watson-Crick base pairs (**A-U**, **G-C**) or wobble base pairs (**U-G**), respectively. Considering only the Watson-Crick and wobble base pair RNA structures, we set the restriction that one vertex can only paired with at most another vertex. Let  $i < r$ , we call arcs  $(i, j)$  and  $(r, s)$  crossing if  $i < r < j < s$  holds. In this representation a pseudoknot-free secondary structure is a diagram without crossing arcs. Otherwise, i.e. diagrams with crossings represent pseudoknot structures. The above mentioned topological folding algorithm, `gfold`, depends crucially on RNA shapes. These are obtained (recursively) by collapsing stacks into arcs and by removing any 1-arc. Shapes are obtained by considering homotopy-classes of arcs and represent thereby the “key” topological information that lies within the original structure, see Figure 1 (B). RNA shapes are the central determinant of the multiple-context free language of topological RNA structures.

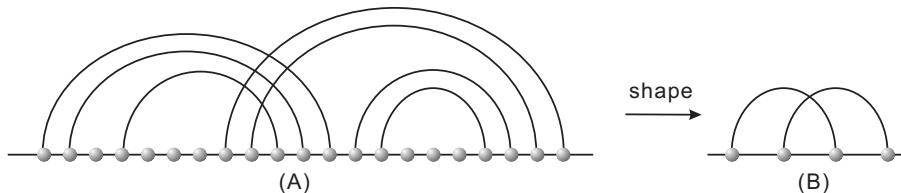
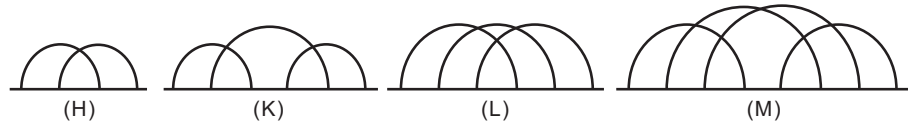


FIGURE 1. From a diagram (A) to its shape (B).

In [17] it identifies a particular topological fact, crucial for folding. That is, for fixed topological genus, there exist only finitely many shapes. This immediately implies that, despite the fact that there are infinitely many RNA structures of fixed topological genus, the generating function can be reduced to a generating polynomial. We shall refer to this polynomial as the shape polynomial. While the situation is fairly easy for genus one [17], see Figure 2, for higher genera it is not trivial to obtain the shapes.

FIGURE 2. The four shapes employed in the topological folding algorithm `gfold`.

$g=1$	2	3	4	5
4	3696	15214144	148120104704	2638025019442176

TABLE 1. The number of shapes of fixed genus  $g$ .

Interestingly, more than 95% of all known RNA-pseudoknot structures are build very “regularly”. They are derived from the aforementioned 4 shapes by means of concatenation and nesting. This observation has led to the notion of  $\gamma$ -structures [5], obtained as concatenation and nesting of shapes of genus less than  $\gamma$ . Thus, despite the fact that the overall genus of  $\gamma$ -structures is arbitrary, they are composed by finitely many blocks of at most genus  $\gamma$ -complexity.

This fits well with what we know about RNA secondary structures: these are build by concatenation and nesting of simple arcs. Topological RNA Structures generalize this in a natural way, utilizing novel building blocks, more complex than simple arcs, i.e. RNA shapes described in the following. The problem is thus reduced to finding and analyzing shapes, whose numbers increase rapidly with increasing genus, see Table 1.

Recently, a linear time uniform random sampler for pseudoknotted RNA structures of given topological genus has been presented [8]. Unfortunately this framework cannot be used for shapes.

In this paper we present a linear time, uniform sampling algorithm for shapes of fixed topological genus. The core idea traces back to a bijection of Chapuy [3], that reduces genus by recursive “splicing” of certain vertices. In difference to the aforementioned uniform sampling [8], the work is based on a specific refinement. Namely, here we keep track of the labeled vertices produced by slicing over many such processes. This enhancement enables us to establish new recursions, which allow us to uniformly generate shapes from trees with a specific number of labeled vertices. The process requires us to characterize which trees actually generate shapes (shape-trees). To this end we show that a bijection of Rémy [18] is compatible with shape-trees and can therefore be restricted. As a result we can give an explicit formula for the coefficients of the shape polynomial.

The paper is organized as follows: in Section 2 we introduce the basic framework. In Section 3 we give an interpretation of the generating function of structures of fixed topological genus based on our refined splicing. The result implies a formula for the  $P_g(z)$  polynomials of [6, 1]. Finally we study the recursion for shapes in Section 4. Here we show that first the original maps restrict naturally to shapes and secondly that Rémy's bijection [18] can be restricted to shape-trees. These two observations allow us to find an explicit formula for the shape polynomial. Finally, in Section 5, we translate the results of Section 4 and derive the linear time, uniform generation algorithm for shapes of fixed topological genus.

## 2. SOME BASIC FACTS

**2.1. Diagrams.** A diagram is a labeled graph over the vertex set  $[n] = \{1, \dots, n\}$  in which each vertex has degree  $\leq 3$ , represented by drawing its vertices in a horizontal line. The backbone of a diagram is the sequence of consecutive integers  $(1, \dots, n)$  together with the edges  $\{\{i, i+1\} \mid 1 \leq i \leq n-1\}$ . The arcs of a diagram,  $(i, j)$ , where  $i < j$ , are drawn in the upper half-plane. We shall distinguish backbone edges  $\{i, i+1\}$  from arcs  $(i, i+1)$ , which we refer to as a 1-arc. Two arcs  $(i, j)$ ,  $(r, s)$ , where  $i < r$  are crossing if  $i < r < j < s$  holds. Parallel arcs of the form  $\{(i, j), (i+1, j-1), \dots, (i+\ell-1, j-\ell+1)\}$  is called a stack, and  $\ell$  is called the length of this stack. Furthermore, the particular arc,  $(1, n)$ , is called the rainbow, see Figure 3 (A).

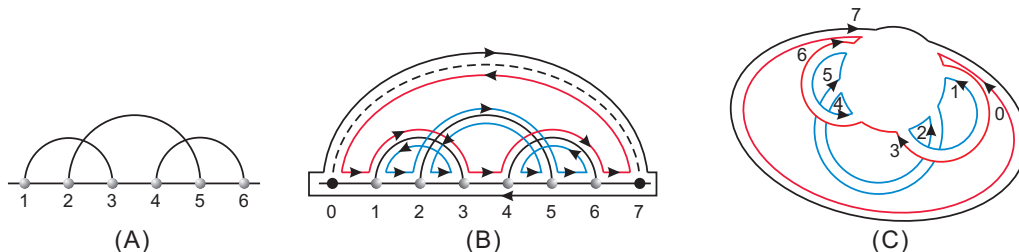


FIGURE 3. (A) A diagram. (B) the fattening of (A) augmented by the rainbow  $(0, 7)$ . Here  $\sigma = (0, 1, 2, 3, 4, 5, 6, 7)$ ,  $\alpha = (0, 7)(1, 3)(2, 5)(4, 6)$ . Accordingly  $\gamma = \alpha \circ \sigma = (0, 3, 6)(1, 5, 4, 2)(7)$  has two cycles. (C) Collapsing the backbone into a vertex.

**2.2. Fatgraphs and unicellular maps.** In this section, we discuss the filtration of diagrams by topological genus. In order to extract topological properties of diagrams those need to be enriched to fatgraphs. The latter are tantamount to a cell-complex of an by construction orientable,

topological surfaces. Formally, we make this transition [1] by “thickening” the edges of the diagram into (untwisted) bands or ribbons. Furthermore each vertex is inflated into a disc. This inflation of edges and vertices means to replace a set of incident edges by a sequence of half-edges. This constitutes the fatgraph  $\mathbb{D}$  [10, 15], see Figure 3 (B).

A fatgraph is thus a graph enriched by a cyclic ordering of the incident half-edges at each vertex and consists of the following data: a set of half-edges,  $H$ , cycles of half-edges as vertices and pairs of half-edges as edges. Consequently, we have the following definition:

**Definition 1.** A fatgraph is a triple  $(H, \sigma, \alpha)$ , where  $\sigma$  is the vertex-permutation and  $\alpha$  a fixed-point free involution.

In the following we will deal with orientable fatgraphs<sup>1</sup>. Each ribbon has two boundaries. The first one in counterclockwise order shall be labeled by an arrowhead, see Figure 3 (B).

A fatgraph  $\mathbb{D}$  exhibits a phenomenon, not present in its underlying graph  $D$ . Namely, one can follow the (directed) sides of the ribbons rotating counterclockwise around the vertices. This gives rise to  $\mathbb{D}$ -cycles or boundary components, constructed by following these directed boundaries from disc to disc. Algebraically, this amounts to form the permutation  $\gamma = \alpha \circ \sigma$ .

In the following we consider only diagrams with a rainbow. As we shall see, the rainbow arc provides a canonical first boundary component, which travels on top of the rainbow arc and the bottom of the backbone of the diagram.

A fatgraph,  $\mathbb{D}$ , can be viewed as a “drawing” on a certain topological surface.  $\mathbb{D}$  is a 2-dimensional cell-complex over its geometric realization, i.e. a surface without boundary,  $X_{\mathbb{D}}$ , realized by identifying all pairs of edges [13]. Key invariants of the latter, like Euler characteristic [13]

$$(2.1) \quad \chi(X_{\mathbb{D}}) = v - e + r,$$

$$(2.2) \quad g(X_{\mathbb{D}}) = 1 - \frac{1}{2}\chi(X_{\mathbb{D}}),$$

where  $v, e, r$  denotes the number of discs, ribbons and boundary components in  $\mathbb{D}$  [13] are defined combinatorially. However, equivalence of simplicial and singular homology [7] implies that these

---

<sup>1</sup>Here ribbons may also be allowed to twist giving rise to possibly non-orientable surfaces [13].

combinatorial invariants are in fact invariants of  $X_{\mathbb{D}}$  and thus topological. This means the surface  $X_{\mathbb{D}}$  provides a topological filtration of fatgraphs.

Since adding a rainbow or collapsing the backbone of a diagram, see Figure 3 (C), does not change the Euler characteristic, the relation between genus and number of boundary components is solely determined by the number of arcs in the upper half-plane:

$$(2.3) \quad 2 - 2g - r = 1 - n,$$

where  $n$  is number of arcs and  $r$  the number of boundary components. The latter can be computed easily and allows us therefore to obtain the genus of the diagram.

**Definition 2.** A unicellular map  $\mathbf{m}$  of size  $n$  is a fatgraph  $\mathbf{m}(n) = (H, \alpha, \sigma)$  in which the permutation  $\alpha \circ \sigma$  is a cycle of length  $2n$ .

While unicellular maps are simply particular fatgraphs, they naturally arise in the context of diagrams, by two observations. First in the diagram one may collapse the backbone into a single vertex. Second the mapping

$$\pi: (H, \sigma, \alpha) \mapsto (H, \alpha \circ \sigma, \alpha),$$

is evidently a bijection between fatgraphs having one vertex and unicellular maps, see Figure 4. The mapping is called the *Poincaré dual* and interchanges boundary components by vertices, preserving topological genus. In the following, we use  $\pi$  to denote the Poincaré dual.

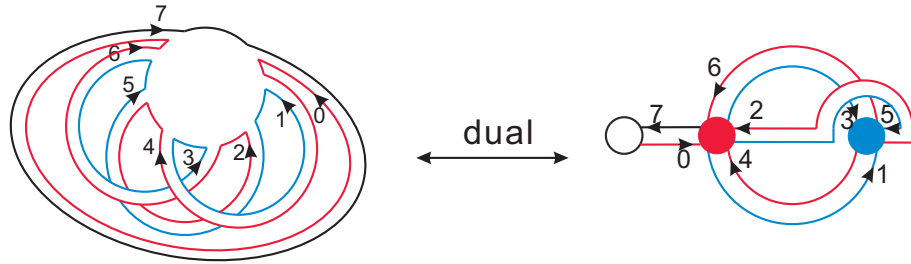


FIGURE 4. The Poincaré dual: we map a fatgraph with 1 vertex and 3 boundary components into a fatgraph with 3 vertexes and 1 boundary component.

Given a unicellular map the permutation  $\sigma$  and  $\gamma$  induces two linear orders of half-edges

$$r <_{\gamma} \gamma(r) <_{\gamma} \dots <_{\gamma} \gamma^{2n-1}(r), \quad r <_{\sigma} \sigma(r) <_{\sigma} \dots <_{\sigma} \sigma^k(r).$$

Let  $a_1$  and  $a_2$  be two distinct half-edges in  $\mathbf{m}$ . Then  $a_1 <_\gamma a_2$  expresses the fact that  $a_1$  appears before  $a_2$  in the boundary component  $\gamma = \alpha \circ \sigma$ . Suppose two half-edges  $a_1$  and  $a_2$  belong to the same vertex  $v$ . Note that  $v$  is effectively a cycle which we assume to originate with the first half-edge along which one enters  $v$  traveling  $\gamma$ . Then  $a_1 <_\sigma a_2$  expresses the fact that  $a_1$  appears (counterclockwise) before  $a_2$ .

The Poincaré dual maps the rainbow into a distinguished vertex of degree one and provides thereby a natural origin for the cycle  $\gamma$ . We call this vertex the *plant*, see Figure 4. Given a unicellular map we call a half-edge the minimum half-edge of a vertex  $v$  if it is the first half-edge via which  $\gamma$  visits  $v$ .

**2.3. Shapes.** An arc is called a 1-arc if it is the form  $(i, i + 1)$ . Two arcs are called parallel if they are of the form of  $(i, j)$  and  $(i + 1, j - 1)$ . A diagram is called a *preshape* if it contains neither 1-arcs nor parallel arcs, see Figure 5. A preshape without a rainbow is called pure. Clearly, there is a projection from preshapes to pure preshapes obtained by removing the latter. A shape is then obtained from a pure preshape by adding a rainbow.

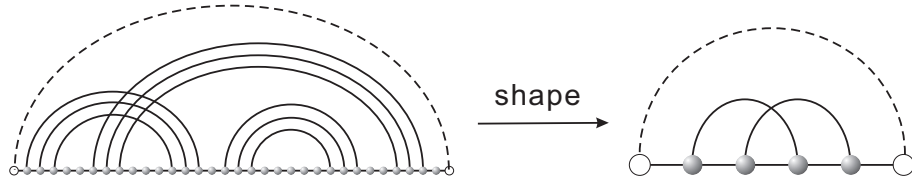


FIGURE 5. From a diagram to a shape by removing all 1-arc and parallel arcs. The dash arc is a rainbow arc, where a preshape is nested inside.

**Proposition 1.** *Let  $S_g$  be a shape of genus  $g$  having  $n$  arcs. Let further  $\mathfrak{s}_g$  denote its associated unicellular map. Then any vertex in  $\mathfrak{s}_g$  has degree  $\geq 3$ .*

*Proof.* We prove the proposition by contradiction. Suppose  $v$  is a vertex in  $\mathfrak{s}_g$ . The boundary component in  $S_g$  associated to  $v$  travels  $d(v)$  arcs. The Poincaré dual maps a boundary component to a vertex, so in case of  $d(v) = 1$ , the boundary component travels only one arc and is thus a 1-arc. A boundary component consisting of two arcs is obtained by either parallel arcs or subsequent arcs, where the endpoint of the second arc travels via the backbone to the start point of the first. The latter case is impossible since a shape always contains a rainbow which increases the size to three and the proposition follows, see Figure 4.  $\square$

**2.4. Topological induction.** In this section we present a construction of [3], which plays a key role for our main result. It consists of two processes: a slicing-map  $\Xi$  and a gluing-map  $\Lambda$ , which, when restricted to the proper classes, are inverse to each other, see Figure 6.

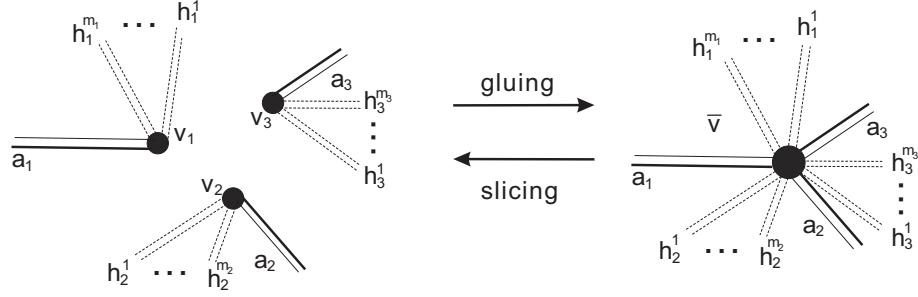


FIGURE 6. Illustration of gluing and slicing in a unicellular map.

The slicing process splits a vertex into  $(2g + 1)$  vertices and thereby reduces the genus of the map by  $g$ . Gluing effectively inverts slicing, namely: gluing any  $(2g + 1)$  vertices in a unicellular map increases the genus of the map by  $g$ . Slicing and gluing preserve unicellularity.

**Definition 3.** A half-edge  $h$  is an *up-step* if  $h <_{\gamma} \sigma(h)$ , and a *down-step* if  $\sigma(h) \leq_{\gamma} h$ .  $h$  is called a *trisection* if  $h$  is a down-step and  $\sigma(h)$  is not the minimum half-edge of its respective vertex.

The number of trisections in a unicellular map is an invariant of a unicellular map with fixed genus  $g$ . Moreover, then number is given by the following lemma:

**Lemma 1.** [3] *Let  $\mathfrak{m}_g$  be a unicellular map of genus  $g$ . Then  $\mathfrak{m}_g$  has exactly  $2g$  trisections.*

Slicing reduces the number of trisections in a unicellular map of genus  $g$ . First we pick up a trisection  $\tau$  and assume it is contained in a vertex  $v$ . Let  $a_1$  denote the minimum half-edge in  $\bar{v}$ , and  $a_3$  denote the half-edge located anticlockwise from  $\tau$ . We consider for the half-edge between  $a_1$  and  $a_3$ ,  $a_2$ , that is the minimum half-edge satisfying  $a_2 >_{\gamma} a_3$ . We can always find such a half-edge  $a_2$  since  $\tau$  is a trisection and  $\tau >_{\gamma} a_3$ , by definition.

Let

$$\bar{v} = (a_1, h_2^1, \dots, h_2^{m_2}, a_2, h_3^1, \dots, h_3^{m_3}, a_3, h_1^1, \dots, h_1^{m_1}),$$



and

$$\bar{\gamma} = (\ell_1^1, \dots, \ell_{k_1}^1, a_1, \ell_1^3, \dots, \ell_{k_3}^3, a_3, \ell_1^2, \dots, \ell_{k_2}^2, a_2, \ell_1^4, \dots, \ell_{k_4}^4).$$

We slice  $\bar{v}$  into three vertices  $v_i$ ,  $i = 1, 2, 3$ , where  $v_i = (a_i, h_i^1, \dots, h_i^{m_i})$ . The new boundary is given by

$$\gamma = (\ell_1^1, \dots, \ell_{k_1}^1, a_1, \ell_1^2, \dots, \ell_{k_2}^2, a_2, \ell_1^3, \dots, \ell_{k_3}^3, a_3, \ell_1^4, \dots, \ell_{k_4}^4).$$

By construction  $a_1$  and  $a_2$  are the minimum half-edges in  $v_1$  and  $v_2$  respectively. However,  $a_3$  is not necessarily minimal in  $v_3$ . If  $a_3$  is the minimum, we have  $a_1$ ,  $a_2$  and  $a_3$  as the minimum half-edges in  $v_1$ ,  $v_2$  and  $v_3$ , respectively. Otherwise,  $\tau$  remains a trisection in  $v_3$ .

Consequently, we have two mappings, depending on whether or not  $a_3$  is minimal:

$$\rho_1: (\bar{\mathbf{m}}, \tau) \rightarrow (\mathbf{m}, v_1, v_2, v_3), \quad \rho_2: (\bar{\mathbf{m}}, \tau) \rightarrow (\mathbf{m}, v_1, v_2, \tau),$$

where  $\mathbf{m}, \bar{\mathbf{m}}$  are unicellular maps of genus  $g$  and  $g + 1$ , respectively.

In the first case,  $\tau$  is no longer a trisection after slicing and called a *Type I*. In the second case,  $\tau$  remains a trisection, a trisection of *Type II*.

**Proposition 2.** [3] *The mappings  $\rho_1$  and  $\rho_2$  are bijections.*

Gluing can be described as follows: given a unicellular map of  $\mathbf{m}_{g-k}$ , together with a sequence of vertices  $V = \{v_1, \dots, v_{2k+1}\}$ , where  $v_i <_{\gamma} v_{i+1}, \forall 1 \leq i < 2k + 1$ , then:

**I.** we glue the last three vertices  $v_{2k-1}$ ,  $v_{2k}$  and  $v_{2k+1}$  via  $\rho_1^{-1}$ , thereby obtaining the unicellular map  $\mathbf{m}_{g-k+1}$  together with a type I trisection  $\tau^I$ .

**II.** we apply  $\rho_2^{-1}(\mathbf{m}_{g-k+i}, v_{2k-2i-1}, v_{2k-2i}, \tau^I)$   $k - 1$  times for  $i = 1$  to  $i = k - 1$ . This produces the unicellular map  $\mathbf{m}_g(n)$ , together with a trisection  $\tau^{II}$ . The process defines a mapping

$$\Lambda(\mathbf{m}_{g-k}, v_1, \dots, v_{2k+1}) = (\mathbf{m}_g, \tau).$$

The order of the vertices in  $V$  is induced by the boundary component,  $\gamma$ . Thus  $V$  can be considered as a set of vertices in  $\mathbf{m}_{g-k}$ , ordered by  $<_{\gamma}$ .  $\Lambda$  merges vertices from right to left by first applying  $\Phi$  once then applying  $\Psi$  until all vertices are glued together.

$\Lambda$  is reversed as follows: given a unicellular map  $\mathbf{m}_g$  of genus  $g$  and  $i = 0$ :

**1.** if  $\tau$  is type II trisection in  $\mathbf{m}_{g-i}$ , then let  $(\mathbf{m}_{g-i-1}, v_{2i+1}, v_{2i+2}, \tau) = \rho_2(\mathbf{m}_{g-i}, \tau)$ . We increase  $i$  to  $i + 1$  and repeat step **1**.

2. if  $\tau$  has type I, let  $(\mathbf{m}_{g-i}, v_{2i+1}, v_{2i+2}, v_{2i+3}) = \rho_1^{-1}(\mathbf{m}_{g-i-1}, \tau)$ .

Then we return

$$\Xi(\mathbf{m}_g, \tau) = (\mathbf{m}_{g-i}, V_\tau).$$

By construction,  $\Lambda$  and  $\Xi$  are inverse to each other.

The bijections  $\Lambda$  and  $\Xi$  immediately induce a connection between unicellular maps having higher genus with those of lower genus.

**Theorem 1.** [3] *Let  $U_g^t$  denote the set of tuples  $(\mathbf{m}_g, v_1, \dots, v_t)$ , where  $v_1, \dots, v_t$  is a sequence of vertices in  $\mathbf{m}_g$ . Furthermore, let  $D_g$  denote the set of tuples  $(\mathbf{m}_g, \tau)$ , where  $\tau$  is a trisection of  $\mathbf{m}_g$ . Then*

$$\Lambda: \bigcup_{k=0}^{g-1} U_k^{2g-2k+1} \rightarrow D_g, \quad \Xi: D_g \rightarrow \bigcup_{k=0}^{g-1} U_k^{2g-2k+1},$$

are bijections and  $\Lambda \circ \Xi = \text{id}$  and  $\Xi \circ \Lambda = \text{id}$ .

The theorem has the following enumerative corollary: let  $\epsilon_g(n)$  denote the number of unicellular map of genus  $g$  having  $n$  edges. Then

**Corollary 1.**

$$(2.4) \quad 2g \cdot \epsilon_g(n) = \binom{n+1-2(g-1)}{3} \epsilon_{g-1}(n) + \dots + \binom{n+1}{2g+1} \epsilon_0(n).$$

Here the  $2g$ -factor on left hand side counts the number of trisection in  $\mathbf{m}_g$  and the binomial coefficients on the right hand side count the number of distinct selections of subsets of  $(2k+1)$  vertices from a unicellular map  $\mathbf{m}_{g-k}$ .

Iterating  $\Xi$ , we obtain

$$(2.5) \quad \epsilon_g(n) = \sum_{0=g_0 < g_1 < \dots < g_r = g} \prod_{i=1}^r \frac{1}{2g_i} \binom{n+1-2g_{i-1}}{2(g_i - g_{i-1}) + 1} \cdot \epsilon_0(n),$$

where  $\epsilon_0(n)$  is the number of planar trees having  $n$  edges, i.e. the Catalan number  $\frac{1}{n+1} \binom{2n}{n}$ .

3. UNICELLULAR MAPS OF GENUS  $g$ 

In Section 2, vertices are labeled with respect to only one iteration. After applying  $\Lambda$  there is a normalization via the factor  $2g$  after which a new labeling is being employed. In this Section we consider a pair consisting of a tree with fixed labeled vertices and a unicellular map of genus  $g$ , also with a fixed set of labelled vertices. We then study the set of glue paths from this tree recruiting exclusively its labelled vertices, which produce the labelled unicellular map.

We begin by considering trees having  $n$  edges and  $k$  labeled vertices,  $\epsilon_0^{(k)}(n)$ . Clearly, the number of these trees is given by the Catalan number  $\text{Cat}(n) = \frac{1}{n+1} \binom{2n}{n}$ , i.e.

$$\epsilon_0^{(k)}(n) = \binom{n+1}{k} \epsilon_0(n) = \binom{n+1}{k} \text{Cat}(n).$$

Next we study the case where  $g > 0$ . Consider a unicellular map  $\mathbf{m}_{g,n}^{(k)}$  with  $k$  labeled vertices. Applying the slicing bijection  $\Xi$  once we produce  $2t+1$  labeled vertices and the genus decreases by  $t$ . Therefore, we obtain a new unicellular map  $\mathbf{m}_{g-t,n}^{(k')}$  where  $k' = k + 2t + 1$ , if in the former we slice an unlabeled vertex and  $k' = k + 2t$ , if we slice a labeled vertex. Then we have the following recursion

$$(3.1) \quad 2g \cdot \epsilon_g^{(k)}(n) = \sum_{t=1}^g \binom{k+2t+1}{2t+1} \epsilon_{g-t}^{(k+2t+1)}(n) + \sum_{t=1}^g \binom{k+2t}{2t+1} \epsilon_{g-t}^{(k+2t)}(n).$$

Suppose we are given a tree  $\mathbf{m}_{0,n}^{(k_0)}$  having  $k_0$  labeled vertices and a unicellular map  $\mathbf{m}_{g,n}^{(k)}$  having  $k$  labeled vertices. In order to construct glue paths from  $\mathbf{m}_{0,n}^{(k_0)}$  to  $\mathbf{m}_{g,n}^{(k)}$  we proceed by induction on  $g$ . The induction basis is clear and by induction hypothesis we have obtained a labeled unicellular map  $\mathbf{m}_{g_1,n}^{(k_1)}$ . The map  $\mathbf{m}_{g_1,n}^{(k_1)}$  can produce two different labeled, unicellular maps, namely  $\mathbf{m}_{g_2}^{(k_1-2(g_2-g_1)+1)}$  or  $\mathbf{m}_{g_2}^{(k_1-2(g_2-g_1))}$ , depending whether we label the new vertex or not. By applying eq. 3.1, we can compute the number of  $\mathbf{m}_{g,n}^{(k)}$  by  $\mathbf{m}_{0,n}^{(k_0)}$  inductively.

Let us first apply the new recursion in order to derive expressions for the generating function of RNA structures of fixed topological genus,  $C_g^{(k)}(z) = \sum_{i=0}^{\infty} \epsilon_g^{(k)}(i) z^i$ .

First we consider the case when  $g = 0$  and  $k = 0$ , i.e., a tree without any labeled vertex. Clearly,  $C_0^{(0)}(z)$  satisfies

$$C_0^{(0)}(z) = z(C_0^{(0)}(z))^2 + 1,$$

whence  $C_0^{(0)}(z) = \frac{1 - \sqrt{1 - 4z}}{2z}$ . For  $k > 0$ , we accordingly have:

**Lemma 2.** *We have*

$$(3.2) \quad C_0^{(k)}(z) = \text{Cat}(k-1)z^{k-1}(1-4z)^{-\frac{2k-1}{2}}, \forall k > 0,$$

where  $\text{Cat}(n)$  denotes the Catalan number  $\text{Cat}(n) = \frac{1}{n} \binom{2n}{n}$ .

*Proof.* A unicellular map of genus 0,  $\mathbf{m}_{0,n}^{(k)}$ , is a planar tree with  $k$  labeled vertices. We decompose  $\mathbf{m}_{0,n}^{(k)}$  starting from its root. Suppose  $v$  is the first vertex we encounter and  $e$  is the leftmost edge of  $v$ . Removing  $e$  we obtain two subtrees, containing  $k_1$  and  $k_2$  labeled vertices, respectively, where  $k_1 + k_2 = k$ . Therefore, the generating function  $C_0^{(k)}(z)$  satisfies

$$(3.3) \quad C_0^{(k)}(z) = \sum_{i=0}^k z \cdot C_0^{(i)}(z) \cdot C_0^{(k-i)}(z), \quad k > 1,$$

and

$$C_0^{(1)}(z) = 1 + z \cdot C_0^{(0)}(z) \cdot C_0^{(1)}(z) + z \cdot C_0^{(1)}(z) \cdot C_0^{(0)}(z).$$

from which  $C_0^{(1)}(z) = (1 - 4z)^{-1/2}$  follows. Furthermore, we observe that  $C_0^{(0)}(z)$  and  $C_0^{(1)}(z)$  satisfy eq. (3.2).

We continue by induction on  $k$ . By induction hypothesis, for  $1 < t < k - 1$ ,  $C_0^{(t)}(z)$  satisfies eq. (3.2). Then solving eq. (3.3) yields

$$C_0^{(k)}(z) = \frac{1}{1 - 2zC_0^{(0)}(z)} \sum_{i=1}^{k-1} z \cdot C_0^{(i)}(z) \cdot C_0^{(k-i)}(z).$$

By assumption, we have  $C_0^{(t)}(z) = \text{Cat}(t-1)z^{t-1}(1-4z)^{-(2t-1)/2}$ ,  $\forall t < k$ , whence

$$\begin{aligned} C_0^{(k)}(z) &= \frac{1}{1 - 2zC_0^{(0)}(z)} z^{k-1}(1-4z)^{-(2k-2)/2} \sum_{i=1}^{k-1} \text{Cat}(i-1)\text{Cat}(k-i-1) \\ &= z^{k-1}(1-4z)^{-(2k-1)/2} \text{Cat}(k-1). \end{aligned}$$

Thus  $C_0^{(k)}(z)$  also satisfies eq. (3.3) and the lemma holds by induction.  $\square$   $\square$

In view of eq. (3.1) and  $C_g^{(k)}(z) = \sum_{i=0}^{\infty} \epsilon_g^{(k)}(i) z^i$  we derive

$$(3.4) \quad 2g \cdot C_g^{(k)}(z) = \sum_{t=1}^g \binom{k+2t+1}{2t+1} C_{g-t}^{(k+2t+1)}(z) + \sum_{t=1}^g \binom{k+2t}{2t+1} C_{g-t}^{(k+2t)}(z).$$

Iterating the recursion of eq. (3.4)  $r$  times we obtain a sequence of tuples  $(g_i, k_i)_{1 \leq i \leq r}$ , where  $g_i$  is the genus of  $\mathfrak{m}_{0,n}^{k_i}$  and  $k_i$  is the respective number of labeled vertices. By construction, we have  $k_i - k_{i-1} = 2(g_i - g_{i-1}) + 1$ , if the new vertex from gluing is not labeled, and  $k_i - k_{i-1} = 2(g_i - g_{i-1})$ , if the new vertex is labeled. Or put differently, whether or not we sliced an unlabelled or a labeled vertex. Let  $t_i = k_i - k_{i-1}$ , then the key information is expressed via the two sequences of integers:

$$g_0 = g_0 < g_1 < \dots < g_r = g, \quad 0 = t_0 = t_1 \leq t_2 \leq \dots \leq t_r = r - t,$$

where  $r$  equals the number of applications of the mapping  $\Xi$ ,  $g_i$  is the genus of  $\mathfrak{m}_{g_i, n}$ . The number  $t_{i+1} - t_i$  is a signature indicating whether we label new vertex or not. In case of  $t_{i+1} - t_i = 1$  we label the newly obtained vertex in the  $i$ th step of gluing, and in case of  $t_{i+1} - t_i = 0$  we do not. Accordingly a glue path between  $\mathfrak{m}_{0,n}^{(k)}$  and  $\mathfrak{m}_{g,n}^{(0)}$  can be reconstructed from the the sequence of pairs  $(g_i, t_i)_{1 \leq i \leq r}$ .

We next employ this construction in order to express the generating function of unicellular maps,  $C_g(z)$  as follows:

**Theorem 2.** *The generating function of unicellular map of genus  $g$  has the form*

$$(3.5) \quad C_g(z) = \sum_{t=0}^{g-1} \kappa_t^{(g)} \cdot \frac{z^{2g+t}}{(1-4z)^{2g+1+t-\frac{1}{2}}},$$

where  $\kappa_t^{(g)} = a_t^{(g)} \text{Cat}(2g+t)$  and

$$(3.6) \quad a_t^{(g)} = \sum_{\substack{0=g_0 < g_1 < \dots < g_r = g \\ 0=t_0 = t_1 \leq t_2 \leq \dots \leq t_r = r-t}} \prod_{i=1}^r \frac{1}{2g_i} \binom{2g+t - (2g_{i-1} + (i-1)) + t_i}{2(g_i - g_{i-1}) + 1}.$$

We present the the coefficients  $\kappa_t^{(g)}$  for genera  $g \leq 5$  in Table 2.

	g=1	2	3	4	5
t=0	1	21	1485	225225	59520825
1		105	18018	4660227	1804142340
2			50050	29099070	18472089636
3				56581525	78082504500
4					117123756750

TABLE 2. Theorem 2: the coefficients  $\kappa_t^{(g)}$ .

*Proof.* Using eq. (3.4), we have

$$\begin{aligned}
C_g(z) &= \frac{1}{2g} \sum_{g_1=0}^{g-1} C_{g_1}^{2(g-g_1)+1}(z) \\
&= \frac{1}{2g} \sum_{g_1=0}^{g-1} \frac{1}{2g_1} \sum_{g_1>g_2} \left( \binom{2(g-g_2)+2}{2(g_1-g_2)+1} C_{g_2}^{2(g-g_2)+2}(z) + \binom{2(g-g_2)+1}{2(g_1-g_2)+1} C_{g_2}^{2(g-g_2)+1}(z) \right) \\
&\quad \vdots \\
&= \sum_{t=0}^{g-1} a_t^{(g)} C_0^{2g+t+1}(z) \\
&= \sum_{t=0}^{g-1} a_t^{(g)} \text{Cat}(2g+t) z^{2g+t} (1-4z)^{-(2g+t+1-\frac{1}{2})} \\
&= \sum_{t=0}^{g-1} \kappa_t^{(g)} z^{2g+t} (1-4z)^{-(2g+t+1-\frac{1}{2})},
\end{aligned}$$

whence the theorem. □ □

In [1], the generating function  $C_g(z)$  has been shown to have the form

$$C_g(z) = \frac{P_g(z)}{(1-4z)^{3g-\frac{1}{2}}},$$

where  $P_g(z)$  is a certain polynomial.

In view of Theorem 2 we have the following expression for the  $P_g(z)$  polynomials:

**Corollary 2.** *The polynomial  $P_g(z)$  is given by*

$$(3.7) \quad P_g(z) = \sum_{t=0}^{g-1} \kappa_t^{(g)} (1-4z)^{g-1-t}.$$

#### 4. SHAPES OF FIXED GENUS

In this section we study shapes of fixed topological genus. Since there are only finitely many shapes for fixed genus  $g$  [17], their generating function is a polynomial. We give an explicit formula for the coefficients of the shape-polynomial, in which the same  $\kappa_i^{(g)}$  coefficients appear as in the generating function of unicellular maps of genus  $g$  in Theorem 2.

We have shown in Section 2 that a shape corresponds to a unicellular map in which each vertex has degree greater than three,  $\mathfrak{s}_{g,n}$ . Applying  $\Xi$  iteratively to  $\mathfrak{s}_{g,n}$  we derive a tree. By construction, any unlabeled vertex in this tree originally comes from  $\mathfrak{s}_{g,n}$  and thus retains its degree.

Let  $\mathbb{S}_{g,n}^{(k)}$ , denote the set of unicellular maps  $\mathfrak{m}_g^{(k)}$  having  $k$  labeled vertices, in which any unlabeled vertex has degree greater than or equal to three. In particular, the set of unicellular maps corresponding to shapes of genus  $g$  having  $n$  edges is  $\mathbb{S}_{g,n}^{(0)}$ . In the following, let  $\mathfrak{s}_{g,n}^{(k)}$  denote an element in  $\mathbb{S}_{g,n}^{(k)}$ .

Since neither  $\Lambda$  nor  $\Xi$  alter unlabelled vertices we have induced bijections

$$\Lambda: (\mathfrak{s}_{g-t,n}^{(k+2t+1)}, V_{2t+1}) \rightarrow (\mathfrak{s}_{g,n}^{(k)}, \tau) \quad \Xi: (\mathfrak{s}_{g,n}^{(k)}, \tau) \rightarrow (\mathfrak{s}_{g-t,n}^{(k+2t+1)}, V_{2t+1}).$$

Indeed,  $\Xi$ , slices a vertex together with a trisection into a sequence of labeled vertices. and thus does not change the degree of unlabeled vertices in the map. Furthermore,  $\Lambda$  glues three or more labeled vertices into one vertex, which has accordingly minimum degree 3.

Let  $\eta_g(n, k)$  denote the cardinality of  $\mathbb{S}_{g,n}^{(k)}$ ,  $k \geq 0$ . In view of the above and eq. (3.4) we have

$$(4.1) \quad 2g \cdot \eta_g(n, k) = \sum_{i=1}^g \binom{k+2i+1}{2i+1} \eta_{g-i}(n, k+2i+1) + \sum_{i=1}^g \binom{k+2i}{2i+1} \eta_{g-i}(n, k+2i),$$

where  $\binom{n}{m} = 0$ , for  $n < m$ .

Due to the compatibility of slicing and gluing with the vertex degree of unlabelled vertices we can conclude

**Proposition 3.** *The number of shapes of genus  $g$  is given by*

$$(4.2) \quad \eta_g(n, 0) = \sum_{t=0}^{g-1} a_t^{(g)} \eta_0(n, 2g + t + 1),$$

where the  $a_t^{(g)}$  are given by eq. (3.6).

*Proof.* Iterating the recursion in eq. 4.1 we reduce the genus. In view of

$$\eta_g(n, 0) = \frac{1}{2g} \sum_{g_1=0}^{g-1} \eta_{g_1}(n, 2(g - g_1) + 1),$$

we then substitute  $\eta_{g_1}(n, 2(g - g_1) + 1)$  using eq. (3.4) and obtain

$$\begin{aligned} \eta_g(n, 0) &= \frac{1}{2g} \sum_{g_1=0}^{g-1} \frac{1}{2g_1} \sum_{g_1 > g_2} \left( \binom{2(g - g_2) + 2}{2(g_1 - g_2) + 1} \eta_{g_2}(n, 2(g - g_2) + 2) \right. \\ &\quad \left. + \binom{2(g - g_2) + 1}{2(g_1 - g_2) + 1} \eta_{g_2}(n, 2(g - g_2) + 1) \right). \end{aligned}$$

Continuing this substitution we arrive at  $\eta_0(n, w)$  for some integer  $w$ . Since in each substitution, the number of labeled vertices increases by either  $2i$  or  $2i + 1$ , we derive

$$\eta_g(n, 0) = \sum_{t=0}^{g-1} a_t^{(g)} \eta_0(n, 2g + t + 1),$$

where the coefficients,  $a_t^{(g)}$ , are given by eq. 3.6. □

At this point we observe that it possible to analyze the terms  $\eta_0(n, 2g + t + 1)$  further. The idea is to “remove” all unlabeled vertices from any partially labelled tree, thereby reducing the recursion to fully labelled trees. The latter are then enumerated by Catalan numbers.

This removal is facilitated by observing that we can restrict the bijection of Rémy to  $\mathbb{S}_{0,n}^{(k)}$ -trees.

To this end, let us first recall Rémy’s bijection for planar trees [18].



**Theorem 3.** Let  $\epsilon_0(n)$  denote the number of planar trees with  $n$  edges. Then we have the recursion

$$(n + 1)\epsilon_0(n) = 2(2n - 1)\epsilon_0(n - 1).$$

The bijection of Theorem 3 associates a planar tree having  $n$  edges and a labeled vertex to a planar tree with  $(n - 1)$  edges with a labeled sector. It is constructed as follows: observing that in a planar tree having  $n$  edges, there are  $n + 1$  vertices and  $2n - 1$  sectors, Rémy's bijection, illustrated in Figure 7, entails two ways of inserting a vertex into a labeled sector. This vertex-insertion generates from a planar tree with  $n - 1$  edges and a labelled sector a planar tree with  $n$  edges and a labelled vertex. The process can be reversed, i.e., a planar tree with  $n$  edges and a labeled vertex can be re-tracked to a planar tree with  $n - 1$  edges and a labeled sector. Depending on the labeled vertex being a leaf or not, one derives a planar tree having two types of labeled sectors.

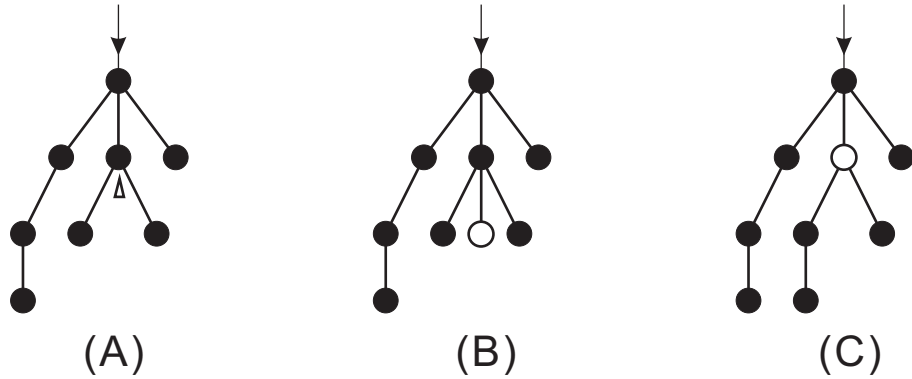


FIGURE 7. Rémy's bijection: two ways of obtaining a planar tree with  $n$  edges and a labeled vertex from a planar tree with  $n - 1$  edges with a labeled sector. We pass from (A) to (B) by inserting a labeled vertex as a leaf to the labeled sector and from (A) to (C) by replacing the vertex containing the sector by the labeled vertex, and carrying the subtree on the left of the sector as its leftmost subtree. This case applies, if the labeled vertex is not a leaf.

We shall prove that Rémy's procedure contracts unlabeled vertices of a  $\mathbb{S}_{0,n+1}^{(k)}$ -tree into a particular type of sector in the resulting  $\mathbb{S}_{0,n}^{(k)}$ -tree. These sectors are referred to as *shape-sector* and are defined as follows: suppose we are given a  $\mathbb{S}_{0,n}^{(k)}$ -tree. A shape-sector is a sector for which Rémy's procedure, inserting a non-leaf unlabeled vertex, generates a  $\mathbb{S}_{0,n+1}^{(k)}$ -tree.

**Lemma 3.** A  $\mathbb{S}_{0,n}^{(k)}$ -tree contains exactly  $(2k - n - 2)$  shape-sectors.

*Proof.* In order to construct a  $\mathbb{S}_{0,n+1}^{(k)}$  from a  $\mathbb{S}_{0,n}^{(k)}$ -tree by Rémy's procedure, we need to ensure that the newly inserted, unlabeled vertex has at least degree 3 and that it does not reduce the degree of the other unlabeled vertex. We shall consider only the insertion not producing a leaf, since it is a vertex of degree 1. Given a sector  $\tau$  in a vertex  $v$ , assume the children of  $v$  are indexed counterclockwise  $v_1 \dots v_m$ , where  $m \geq 2$ . The sector  $\tau$  partitions the  $v$ -children into two blocks:

$$\{v_1 \dots, v_\ell\} \quad \text{and} \quad \{v_{\ell+1} \dots, v_m\}.$$

We make two observations: (a) the newly inserted vertex has at least degree three if  $\{v_{\ell+1} \dots, v_m\} \neq \emptyset$ , see Figure 8. (b) the vertex, that is pushed "down" by the newly inserted vertex retains degree  $\geq 3$ , if and only if  $\ell \geq 2$ , i.e. if  $\tau$  is to the right of the second  $v$ -child in counterclockwise order. The latter applies by construction only to the case where the pushed-down vertex is unlabeled.

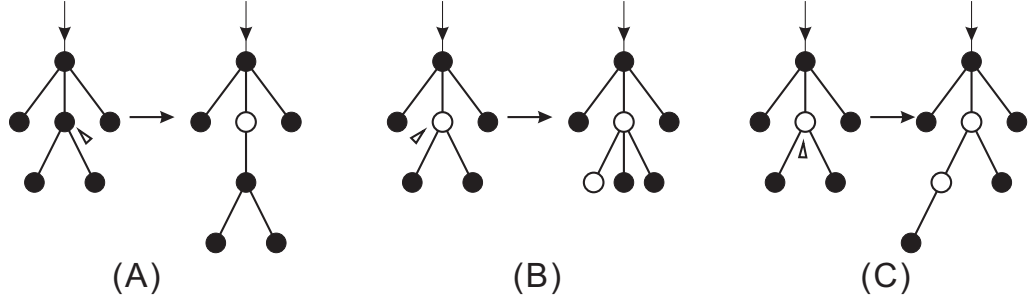


FIGURE 8. How to construct non shape-sectors via Rémy's-procedure. The following insertions produce an unlabeled vertex of degree 2: (A) the sector is in a labeled vertex and  $\{v_{\ell+1} \dots, v_m\} = \emptyset$ , and (B) ( $\ell = 0$ ) and (C) ( $\ell = 1$ ) if the sector is in an unlabeled vertex.

Therefore, a sector in a vertex  $v$  is a shape-sector if and only if

- $\tau$  has the property  $\{v_{\ell+1} \dots, v_m\} \neq \emptyset$ ,
- if  $v$  is unlabeled,  $\tau$  satisfies furthermore  $|\{v_1, \dots, v_\ell\}| \geq 2$ .

There are in total  $2n + 1$  sectors in a tree. The first criterion rules out  $n + 1$  sectors, since each vertex has one such sector. The second criterion rules out 2 sectors from an unlabeled vertices and there are  $n + 1 - k$  of them. Accordingly, the number of shape-sectors is given by

$$2n + 1 - (n + 1) - 2(n + 1 - k) = 2k - n - 2.$$

Any of the  $2k - n - 2$  shape preserved sectors produces a  $\mathbb{S}_{0,n+1}^{(k)}$ -tree by Rémy's procedure, when inserting a non-leaf vertex and the lemma follows.  $\square$

**Corollary 3.** *Let  $\tau$  denote a shape preserved sector and  $\mathbf{m} \in \mathbb{S}_{0,n}^{(k)}$ . Then*

$$\rho: (\mathbf{m}, \tau) \rightarrow (\mathbf{m}', v)$$

is a bijection, where  $v$  is an unlabeled vertex in  $\mathbf{m}'$  and  $\mathbf{m}' \in \mathbb{S}_{0,n+1}^{(k)}$ . In particular we have

$$\begin{aligned} (2k - n - 2)\eta_0(n, k) &= (n + 1 - k)\eta_0(n + 1, k) \\ \eta_0(n, k) &= \binom{2k - (k - 1) - 2}{n + 1 - k} \eta_0(k - 1, k) = \binom{k - 1}{n + 1 - k} \text{Cat}(k - 1). \end{aligned}$$

*Proof.* The corollary follows by restriction of Rémy's bijection. This bijection implies that the removal of an unlabeled vertex of a  $\mathbb{S}_{0,n}^{(k)}$ -tree produces a shape-sector. Furthermore, the order of such removals is irrelevant. Therefore, a  $\mathbb{S}_{0,n}^{(k)}$ -tree can be constructed from a  $\mathbb{S}_{0,m-1}^{(k)}$ -tree together with  $(2k - n + 1)$  shape preserved sectors. Clearly, the number of  $\mathbb{S}_{0,k-1}^{(k)}$ -trees equals  $\text{Cat}(k - 1)$ , where  $\text{Cat}(n)$  is the  $n$ -th Catalan number given by  $\frac{1}{n+1} \binom{2n}{n}$ . To obtain a  $\mathbb{S}_{0,n}^{(k)}$ -tree, we need to insert  $n + 1 - k$  unlabeled vertices. Choosing  $n + 1 - k$  out of  $2k - (k - 1) - 2$  shape preserved sectors from  $\mathbb{S}_{0,k-1}^{(k)}$ , we derive

$$\eta_0(n, k) = \binom{2k - (k - 1) - 2}{n + 1 - k} \eta_0(k - 1, k) = \binom{k - 1}{n + 1 - k} \text{Cat}(k - 1),$$

whence the corollary.  $\square$

In particular, the number of shape-sectors decreases by 1, upon insertion of one, unlabeled vertex and there are at most  $2k - (k - 1) - 2 = k - 1$  insertions into a fully labeled tree having  $n$  edges. This provides another proof that for fixed topological genus there are only finitely many shapes.

We next compute the shape polynomial  $S_g(z) = \sum_n s_g(n)z^n$  where  $s_g$  is the number of shapes having  $n$  arcs. Note that  $s_g(n) = \eta_g(n, 0)$ .

**Theorem 4.** *The shape generating function is given by*

$$(4.3) \quad S_g(z) = \sum_{t=0}^{g-1} \kappa_t^{(g)} z^{2g+t} (1+z)^{2g+t},$$

where  $\kappa_t^{(g)} = a_t^{(g)} \text{Cat}(2g + t)$ .

*Proof.* Since  $s_g(n) = \eta_g(n, 0)$  we have

$$S_g(z) = \sum_n \eta_g(n, 0) z^n = \sum_n \left( \sum_{t=0}^{g-1} a_t^{(g)} \eta_0(n, 2g+t+1) \right) z^n.$$

By Corollary 3 we can express the terms  $\eta_0(n, 2g+t+1)$ ,

$$\begin{aligned} S_g(z) &= \sum_n \left( \sum_{t=0}^{g-1} a_t^{(g)} \eta_0(n, 2g+t+1) \right) z^n \\ &= \sum_n \sum_{t=0}^{g-1} a_t^{(g)} \binom{2g+t}{n-(2g+t)} \text{Cat}(2g+t) z^n \\ &= \sum_{t=0}^{g-1} \kappa_t^{(g)} \left( z^{2g+t} \sum_{n=2g+t}^{2(2g+t)} \binom{2g+t}{n-(2g+t)} z^{n-(2g+t)} \right) \\ &= \sum_{t=0}^{g-1} \kappa_t^{(g)} z^{2g+t} (1+z)^{2g+t}, \end{aligned}$$

where  $\kappa_t^{(g)} = a_t^{(g)} \cdot \text{Cat}(2g+t)$ . □

## 5. UNIFORM GENERATION

In this section we present an algorithm that generates shapes of fixed genus  $g$ . Since the generating function of shapes is a polynomial, a shape of fixed topological genus has only finitely many arcs. In fact we have  $2g \leq n \leq 3g-1$ . The probability of having exactly  $n$  arcs in a shape of fixed genus  $g$  is given by

$$(5.1) \quad \mathbb{P}_g(n) = \frac{s_g(n)}{\sum_{t=0}^{g-1} s_g(2g+t)},$$

where  $s_g(n)$  is the coefficients in  $S_g(z)$ . In the following we generate shapes of fixed topological genus  $g$  and fixed number of arcs  $n$ , where  $2g \leq n \leq 3g-1$ .

In Section 4 we have shown that a shape of genus  $g$  is obtained by gluing  $k$  labeled vertices contained in a partially labelled tree having  $n$  edges, where  $2g+1 \leq k \leq 3g$ . Furthermore, this partially labelled tree is constructed by Rémy's bijection restricted to shape-sectors. The corresponding

probability of this event reads

$$\mathbb{P}_g(n, k) = \frac{a_{k-2g-1}^{(g)} \eta_0(n, k)}{\sum_{t=0}^{g-1} a_t^{(g)} \eta_0(n, 2g+t+1)}.$$

The algorithm generates a shape of genus  $g$  in three steps:

- first we uniformly generate a tree with  $k$  vertices [4],
- secondly we insert  $n+1-k$  unlabeled vertices by Rémy's procedure in shape-sectors. Since all vertices in the tree are labeled, there are  $k-1$  shape-sectors. We then uniformly select  $n+1-k$  from the  $k-1$  shape-sectors and insert unlabeled vertices by Rémy's procedure. The probability of a particular selection is given by  $1/\binom{k-1}{n+1-k}$ ,
- thirdly we select uniformly a particular glue path. In Section 4 we established the trace, i.e. a sequence of pairs  $(g_i, t_i)$ , such that  $g_i < g_{i+1}$  and  $t_{i+1} - t_i$  being equal to either 0 or 1. Suppose the number of labeled vertices is  $k$  and  $t = k - 2g - 1$ . We construct the sequence inductively, with initial status  $(g_0 = 0, t_0 = 0)$  and terminate in case of  $(g_r = g, t_r = r - t)$  for some integer  $r$ . Let

$$\mathbb{P}_{\text{step}}(i|i-1) = \frac{1}{2g_i} \cdot \binom{2g+t-(2g_{i-1}+(i-1))+t_i}{2(g_i-g_{i-1})+1}.$$

Then we have

$$\begin{aligned} & \mathbb{P}((g_i, t_i)|(g_{i-1}, t_{i-1})) = \\ & \frac{\mathbb{P}_{\text{step}}(i|i-1) \cdot \sum_{\substack{g_{i+1} < \dots < g_r = g \\ t_{i+1} \leq \dots \leq t_r = r-t}} \prod_{\ell=i+1}^r \frac{1}{2g_\ell} \binom{2g+t-(2g_{\ell-1}+(\ell-1))+t_\ell}{2(g_\ell-g_{\ell-1})+1}}{\sum_{\substack{g_i < \dots < g_r = g \\ t_i \leq \dots \leq t_r = r-t}} \prod_{\ell=i}^r \frac{1}{2g_\ell} \binom{2g+t-(2g_{\ell-1}+(\ell-1))+t_\ell}{2(g_\ell-g_{\ell-1})+1}}. \end{aligned}$$

We accordingly derive

$$\begin{aligned} & \prod_{i=1}^r \mathbb{P}((g_i, t_i)|(g_{i-1}, t_{i-1})) = \\ & \frac{\prod_{i=1}^r \mathbb{P}_{\text{step}}(i|i-1)}{\sum_{\substack{0=g_0 < g_1 < \dots < g_r = g \\ 0=t_0=t_1 \leq t_2 \leq \dots \leq t_r = r-t}} \prod_{i=1}^r \frac{1}{2g_i} \binom{2g+t-(2g_{i-1}+(i-1))+t_i}{2(g_i-g_{i-1})+1}}. \end{aligned}$$

- finally we realize the  $(g_i, t_i)_i$ -glue path by selecting vertices. Suppose we have at step  $i-1$  the labeled shape  $\mathfrak{s}_{g_{i-1}, n}^{(k_{i-1})}$ . Then we select  $2(g_i - g_{i-1}) + 1$  from the  $k_{i-1}$  labeled vertices uniformly and glue them via  $\Lambda$ . There are  $\binom{2g+t-2(g_{i-1}+(i-1))+t_i}{2(g_i-g_{i-1})+1}$  ways to choose these vertices uniformly, which generates the  $\mathfrak{s}_{g_i, n}^{(k_i)}$  together with a labeled trisection. Since

there are exactly  $2g_i$  trisections in  $\mathfrak{s}_{g_i, n}^{(k_i)}$ , there are  $2g_i$  glue paths generating the same configuration. Therefore, erasing the label of the trisections induces each glue path with a  $1/2g_i$  factor. Accordingly there are

$$\prod_{i=1}^r \mathbb{P}_{\text{step}}(i|i-1)$$

paths with trace  $((g_i, t_i))_{i=1}^r$  from a fixed  $\mathfrak{s}_{0, n}^{(2g+t)}$  to  $\mathfrak{s}_{g, n}^{(0)}$ .

$$\frac{\prod_{i=1}^r \mathbb{P}((g_i, t_i)|(g_{i-1}, t_{i-1}))}{\prod_{i=1}^r \mathbb{P}_{\text{step}}(i|i-1)} = \frac{1}{a_t^{(g)}}.$$

The above process can be formally expressed as follows:

---

**Algorithm 1**


---

```

1: UniformShape (TargetGenus)
2:  $n \leftarrow \text{NumberOfArcs}(g)$ 
3:  $k \leftarrow \text{NumberOfLabel}(n, g)$ 
4:  $t \leftarrow k - 2g$ 
5:  $\mathfrak{s}_{0, k-1} \leftarrow \text{UnifomTree}(k - 1)$ 
6:  $\mathfrak{s}_{0, n}^{(2g+t)} \leftarrow \text{InsertUnlabeled}(\mathfrak{s}_{0, k-1}, n - k + 1)$ 
7:  $i \leftarrow 1$ 
8:  $(g_0, t_0) \leftarrow (0, 0)$ 
9: while  $g_i \leq \text{TargetGenus}$  do
10:    $(g_i, t_i) \leftarrow \text{NextGenus}((g_j, t_j)_{0 \leq j < i}, \text{TargetGenus})$ 
11:    $i \leftarrow i + 1$ 
12: end while
13:  $i \leftarrow 1$ 
14: while  $g_i \leq \text{TargetGenus}$  do
15:    $V_{i-1} \leftarrow \text{SelectVertex}(\mathfrak{s}_{g_{i-1}, n}^{(2g+t-(2g_{i-1}+(i-1))+t_i)}, 2(g_i - g_{i-1}) + 1)$ 
16:    $\mathfrak{s}_{g_i, n}^{(2g+t-(2g_i+(i))+t_{i+1})} \leftarrow \text{Glue}(\mathfrak{s}_{g_{i-1}, n}^{(2g+t-(2g_{i-1}+(i-1))+t_i)}, V_i, t_{i+1})$ 
17:    $i \leftarrow i + 1$ 
18: end while
19: return  $\mathfrak{s}_{g, n}^{(0)}$ 

```

---

The next proposition is implied by Proposition 3 and Corollary 3:

**Proposition 4.** *The probability of a shape generated by Algorithm 1 is  $1/\eta_g(n, 0)$ , i.e. the algorithm generates shapes of genus  $g$  uniformly.*

*Proof.* By construction, the probability of arriving at  $\mathfrak{s}_{g,n}^{(0)}$  from  $\mathfrak{s}_{0,n}^{(2g+t)}$  is given by  $1/a_t^{(g)}$ . The probability to glue from a  $\mathfrak{s}_{0,n}^{(2g+t)}$ -shape equals  $\mathbb{P}_{g,n}(k)$  and is a result of eq. (4.2). In view of Corollary 3, which expresses  $\eta_0(n, k)$  as  $\binom{k-1}{n+1-k} \text{Cat}(k-1)$ , the probability of a particular shape  $\mathfrak{s}_{g,n}^{(0)}$ , generated by Algorithm 1 is given by

$$\begin{aligned} \mathbb{P}(\mathfrak{s}_{g,n}^{(0)}) &= \mathbb{P}_{g,n}(k) \cdot \frac{1}{\text{Cat}(k-1)} \cdot \frac{1}{\binom{k-1}{n+1-k}} \cdot \frac{1}{a_t^{(g)}} \\ &= \frac{a_t^{(g)} \eta_0(n, k)}{\sum_{t=0}^{g-1} a_t^{(g)} \eta_0(n, 2g+t+1)} \cdot \frac{1}{\text{Cat}(k-1) \binom{k-1}{n+1-k}} \cdot \frac{1}{a_t^{(g)}} \\ &= \frac{1}{\sum_{t=0}^{g-1} a_t^{(g)} \eta_0(n, 2g+t+1)} \\ &= \frac{1}{\eta_g(n, 0)}. \end{aligned}$$

□

## 6. DISCUSSION

In this paper, we studied shapes of RNA structures. While topologically motivated by taking homotopy classes of arcs, shapes have a simple combinatorial interpretation and there are, for fixed genus, only finitely many of them.

Topological folding algorithms like [17] show that shapes determine the grammar of the multiple-context free language of topological RNA structures of fixed topological genus. It is therefore of interest to compute shapes of genus  $g$ , effectively. This connection also makes concrete how the topology of RNA structures characterizes their language and reiterates the fact that RNA shapes carry genuinely key information of RNA structures.

Two questions immediately arise. First, can we compute the generating polynomial for arbitrary topological genus with preferably explicit expressions for the coefficients. The latter are of significance as they represent the number of shapes of genus  $g$  with  $n$  arcs. Secondly, can we actually

generate these shapes—i.e. how do they look like as diagrams? This allows us to derive a plethora of nontrivial statistics of shape. Both questions are answered affirmatively in this paper.

As for the first, in Section 4, Theorem 4 we compute the shape polynomial for fixed topological genus. As for the second, we specify in Section 5 an algorithm that uniformly generates shape of fixed genus  $g$  in linear time. We also implement Algorithm 1 and its source code is available at

<http://imada.sdu.dk/~duck/shape.c>

To illustrate uniformity, we display in Figure 9 the multiplicities of shapes of genus 2 obtained by Algorithm 1 and the Binomial coefficients  $\binom{N}{\ell}(1/\sigma_2)^\ell(1 - 1/\sigma_2)^{N-\ell}$ .

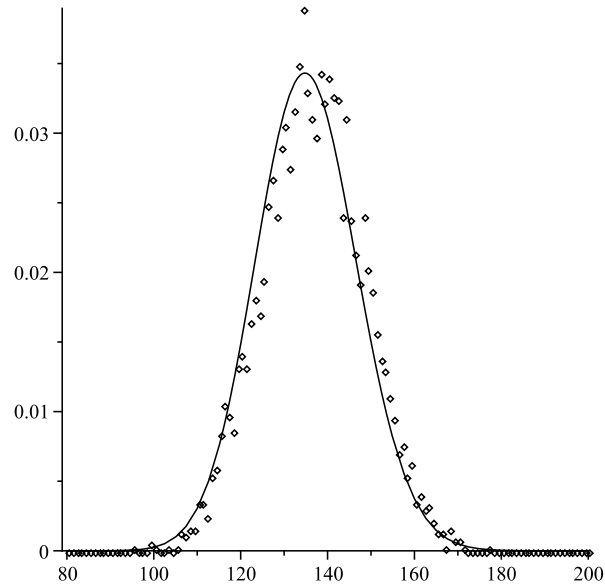


FIGURE 9. Uniform generation of shapes: We generate  $N = 5 \times 10^5$  shapes and display the frequencies of their multiplicities (dots) together with the Binomial coefficients of the uniform sampling  $\binom{N}{\ell}(1/\sigma_2)^\ell(1 - 1/\sigma_2)^{N-\ell}$  (solid curve), where  $\sigma_2 = 3696$  is the number of shapes of genus 2.



We next discuss how to use shapes in order to extract key information from databases. Let us begin with an experiment: we uniformly sample RNA structures of length 200 having genus 2 and study the frequencies of their associated shapes. We observe that first shapes of the same length remains uniformly distributed, see Figure 10 (A). Secondly, the distribution of shapes of different length follows the distribution of the coefficients in the shape polynomial, see Figure 10 (B).

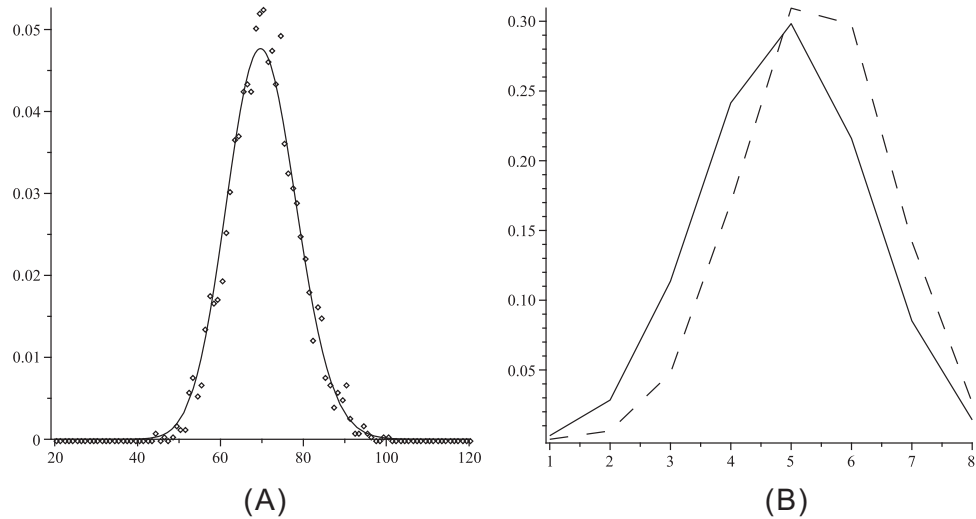


FIGURE 10. Uniform sampling of structures of length 200 of genus 2, (over  $5 \times 10^5$  in total) and display: the multiplicities of shapes with length 16 (A) and the multiplicities of shapes of different lengths (B). The solid curve displays the distribution induced by the coefficients of the shape polynomial, while the dash curve displays the distribution of the sampling process.

This observation motivates to extract such shape multiplicities from a database of RNA-structures and to use this in order to generate RNA structures from shapes using the latter, see Figure 11, where we display the number of RNA pseudoknot structures (PKB1–PKB304) found in Pseudobase [21] having a particular shape. This idea allows to reduce database information succinctly in form of a novel polynomial whose coefficients are the multiplicities of shapes of fixed length. In particular, in case of uniform RNA structures this method would recover the shape polynomial itself.

While the uniform generation algorithm of shapes is of best possible time complexity, it does generate, strictly speaking, *labeled* shapes. That is, shapes with a distinct trisection. Our next objective

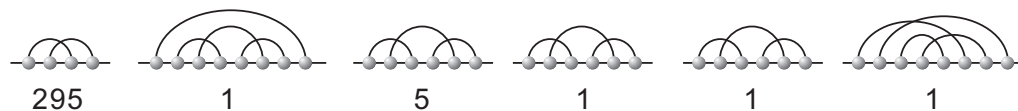


FIGURE 11. Shape-multiplicities of Pseudobase PKB1-PKB304 [21].

is to work on obtaining fully bijective construction methods for unlabeled shapes, i.e. explicit algorithms that derive inductively shapes without encountering the multiplicity  $2g$ . Ultimately this does not matter for applications (nor the time complexity) of the uniform generation *per se* since each labeled shape is generated with the same, finite, multiplicity ( $2g$ ). However, it would be interesting to identify a construction method for unlabeled shapes.

## 7. ACKNOWLEDGMENTS.

We acknowledge the financial support of the Future and Emerging Technologies (FET) programme within the Seventh Framework Programme (FP7) for Research of the European Commission, under the FET-Proactive grant agreement TOPDRIM, number FP7-ICT-318121.

## REFERENCES

- [1] J. E. Andersen, R. C. Penner, C. M. Reidys, and M. S. Waterman. Topological classification and enumeration of RNA structures by genus. *J. Math. Biol.*, 67(5):1261–78, 2013.
- [2] Michael Bon, Graziano Vernizzi, Henri Orland, and A. Zee. Topological classification of RNA structures. *J. Mol. Biol.*, 379:900–911, 2008.
- [3] G. Chapuy. A new combinatorial identity for unicellular maps, via a direct bijective approach. *Adv. Appl. Math.*, 47(4):874–893, 2011.
- [4] P. Duchon, P. Flajolet, G. Louchard, and G. Schaeffer. Boltzmann samplers for the random generation of combinatorial structures. *Combinatorics, Probability and Computing*, 13:2004, 2004.
- [5] H. S. W. Han, T. J. X. Li, and C. M. Reidys. Combinatorics of  $\gamma$ -structures. *J. Comp. Biol.*, page arXiv:1112.4151, 2013.
- [6] J. Harer and D Zagier. The euler characteristic of the moduli space of curves. *Inv. Math.*, 85(3):457–485, 1986.
- [7] A. Hatcher. *Algebraic Topology*. Cambridge University Press, 2002.
- [8] F. Huang, C. M. Reidys, and M. E. Nebel. Generation of rna pseudoknot structures with topological genus filtration. *Math. Biosci.*, 245(2):216C225, 2013.

- [9] D. Konings and R. Gutell. A comparison of thermodynamic foldings with comparatively derived structures of 16s and 16s-like rRNAs. *RNA*, 1:559–574, 1995.
- [10] M. Loebl and I. Moffatt. The chromatic polynomial of fatgraphs and its categorification. *Adv. Math.*, 217:1558–1587, 2008.
- [11] A. Loria and T. Pan. Domain structure of the ribozyme from eubacterial ribonuclease. *RNA*, 2:551–563, 1996.
- [12] R. B. Lyngsø and C. N. Pedersen. RNA pseudoknot prediction in energy-based models. *J. Comp. Biol.*, 7:409–427, 2000.
- [13] W. S. Massey. *Algebraic Topology: An Introduction*. Springer-Verlag, New York, 1967.
- [14] H. Orland and A. Zee. RNA folding and large  $n$  matrix theory. *Nuclear Physics B*, 620:456–476, 2002.
- [15] R. C. Penner, Michael Knudsen, Carsten Wiuf, and Jørgen Ellegaard Andersen. Fatgraph models of proteins. *Comm. Pure Appl. Math.*, 63:1249–1297, 2010.
- [16] R. C. Penner and M. S. Waterman. Spaces of RNA secondary structures. *Adv. Math.*, 101:31–49, 1993.
- [17] C. M. Reidys, F. Huang, J. E. Andersen, R. C. Penner, P. F. Stadler, and M. E. Nebel. Topology and prediction of RNA pseudoknots. *Bioinformatics*, 27:1076–1085, 2011.
- [18] J. L. Rémy. Un procédé itératif de dénombrement d’arbres binaires et son application à leur génération aléatoire. *RAIRO Inform. Théor.*, 19(2):179C195, 1985.
- [19] Elena Rivas and Sean R. Eddy. A dynamic programming algorithm for RNA structure prediction including pseudoknots. *J. Mol. Biol.*, 285:2053–2068, 1999.
- [20] David W Staple and Samuel E Butcher. Pseudoknots: RNA structures with diverse functions. *PLoS Biol.*, 3:e213, 2005.
- [21] Michela Taufer, Abel Licon, Roberto Araiza, David Mireles, F. H. D. van Batenburg, Alexander Gulyaev, and Ming-Ying Leung. PseudoBase++: an extension of PseudoBase for easy searching, formatting and visualization of pseudoknots. *Nucleic Acids Res.*, 37:D127–D135, 2009.
- [22] C. Tuerk, S. MacDougall, and L. Gold. RNA pseudoknots that inhibit human immunodeficiency virus type 1 reverse transcriptase. *Proc. Natl. Acad. Sci. USA*, 89(15):6988–6992, 1992.
- [23] E. Westhof and L. Jaeger. RNA pseudoknots. *Curr. Opin. Struct. Biol.*, 2:327–333, 1992.
- [24] D. Zagier. On the distribution of the number of cycles of elements in symmetric groups. *Nieuw Arch. Wisk. IV*, 13:489–495, 1995.

DEPARTMENT OF MATHEMATICS AND COMPUTER SCIENCE, UNIVERSITY OF SOUTHERN DENMARK, CAMPUSVEJ 55, DK-5230 ODENSE M, DENMARK, TEL.\*: +45-24409251, FAX\*: +45-65502325, E-MAIL\*: DUCK@SANTAFE.EDU